



Simplified kilogram traceability for high-power laser measurement using photon momentum radiometers

KYLE A. ROGERS,^{1,*}  PAUL A. WILLIAMS,¹ GORDON A. SHAW,² AND JOHN H. LEHMAN¹

¹National Institute of Standards and Technology, 325 Broadway, Boulder, Colorado 80305, USA

²National Institute of Standards and Technology, 100 Bureau Dr, Gaithersburg, Maryland 20899, USA

*Corresponding author: kyle.rogers@nist.gov

Received 18 June 2020; revised 7 September 2020; accepted 7 September 2020; posted 9 September 2020 (Doc. ID 399989); published 28 September 2020

Photon momentum radiometers measure the force imparted by a reflected laser beam to determine the laser's optical power. This requires high-accuracy calibration of the force sensors using milligram and microgram mass artifacts. Calibrated test masses can therefore be used to provide traceability of these radiometers to the International System of Units, but low-noise calibration at these mass levels is difficult. Here, we present the improvement in calibration capability that we have gained from implementing a robotic mass delivery system. We quantify this in terms of the specific nuances of force measurements as implemented for laser power metrology. © 2020 Optical Society of America

<https://doi.org/10.1364/AO.399989>

1. INTRODUCTION

Radiation pressure-based laser power meters have proven to be advantageous as high-accuracy primary standards for measuring continuous-wave (CW) laser power above 1 kW [1]. These devices, which we refer to in general as photon momentum radiometers (PMRs) have a distinct convenience in portability. Typical thermal-based primary standard power meters at multikilowatt power levels and above are by necessity large, with limited portability. This is due to thermal techniques requiring a large thermal mass (all the incident laser power must be absorbed), which necessitates high heat capacities and thus large power meter volumes. However, as a nonabsorbing technique, radiation pressure-based laser power meters need not scale in volume with laser power measurement capacity, making them easily portable, even for power levels up to 100 kW.

The portability of these multikilowatt primary standards requires consideration of a portable means of establishing traceability to the International System of Units (SI). Radiation pressure-based laser power meters are traceable to fundamental physical constants through the base units of the meter, kilogram, and second [2]. The most important element in their traceability chain is the calibration of the analytical balance that is responsible for the measurement of force. By nature, a force balance compares forces, be it a mass comparator that determines the relative difference between two masses, or a primary standard such as a Kibble balance [3] or electrostatic force balance [4] that compares the local gravitational force on a

mass to electrically generated forces. The standard and modified commercial force balances that underly each PMR compare the force due to photon momentum and an electromagnetic compensation force calibrated by a mass artifact. In this work, we demonstrate that a PMR can effectively be calibrated in the field by weighing a reference mass, thus allowing simplified periodic calibration of the instrument. Such a calibration could be carried out by the user or a third-party laboratory without the need of high-power laser facilities and high-power standards, which is radically different from convention [5].

To demonstrate this concept, we have assembled a robotic apparatus suitable for calibrating commercial force sensors, incorporating the mass range appropriate to laser power measurements. Here we describe this instrument and its operation. Our purpose is to facilitate its duplication for field calibration of radiation pressure-based laser power meters.

2. BACKGROUND

Radiation pressure-based power measurement can be described as a “nondestructive” measurement method—that is, the laser light is measured based on its reflection rather than its absorption, allowing the beam to continue propagating. In this measurement technique, laser light reflects from a mirror that produces a change in the momentum of the photons comprising the laser beam, and thus imparts a force on the mirror. The relationship between the force F and power P of a laser beam incident on the mirror at an angle θ is described by

$$F = \frac{2rP\cos(\theta)}{c}, \quad (1)$$

where $r = R + (1 - R)\alpha/2$, R is the mirror reflectivity, α is the fraction of nonreflected light absorbed by the mirror, and c is the speed of light.

Constructed in multiple geometries, PMR devices have become a fast and convenient means of power measurement. One configuration is the radiation pressure power meter (RPPM) shown in Fig. 1(a), which has been validated at CW laser powers up to 50 kW [6]. It has also been used to calibrate other high-power thermal detectors [7]. This device has an expanded uncertainty of 1.6% for power levels of 1 kW and above. An alternative geometry, the axial force radiometer (AFR), shown in Fig. 1(b), is a different design in which the incoming laser beam exits the device along the original beam axis [8,9]. This device has been tested at power levels up to 10 kW CW and is also suitable for higher power levels. These devices use high-reflectivity mirrors optimized for the specific angle of incidence at a wavelength of 1070 nm. Highly reflective optics (reflectivity between 0.99998 and 0.99999) allow for minimal absorption, transmission, and diffuse reflectance, which would lead to measurement inequivalence.

Each of the two devices incorporates a precision balance with a manufacturer-specified readability (minimum measurable change in mass) of 1 μg for the AFR and 10 μg for the RPPM. Both balances have specified repeatability and linearity of 0.05 mg or less. The RPPM force sensor is designed such that it can function in both the horizontal and vertical orientation, for variation between calibration and power measurement. The standard uncertainty (0.21%) from this orientation change is included in the expanded 1.6% device uncertainty. The AFR design allows flexibility in the choice of force sensor. A variety of commercial precision balances may be used, provided sufficient resolution and a maximum sensing weight sufficient to support the sensing mirror. Calibration of the force sensor is required to provide SI traceability through the kilogram using the relationship $F = mg \cos \Omega$, where m is the mass of the calibration artifact, g is the local gravitational acceleration, and Ω is the angle of the sensing mirror surface relative to the perpendicular of gravity. Measurement errors due to variations in the acceleration due to gravity g based on geographic location have been considered. Such variations in g do not affect laser power measurements because the sensor measures force directly (not mass). Therefore, we require an accurate local value of g only during calibration (when relating measured force to a reference mass). The PMR mass calibrations described here were

carried out in Boulder, Colorado and we used the local value of $g = 9.801 \text{ m/s}^2$ [10]. Errors due to air buoyancy have also been considered. The relative error on our mass calibration due to air buoyancy is given by the ratio of the densities of air and aluminum (the material comprising the mass artifacts). This ratio has a negligibly small value of 0.0004 and can be ignored.

As an example of the mass range needed for calibration, the force produced by a 1 kW incident laser beam on a highly reflective mirror at a 45° angle of incidence is 4.7 μN . To calibrate a force sensor for operation at this level, we perform calibrations at forces from well above this minimum value down to $\sim 1.5 \mu\text{N}$. This minimum corresponds to a mass of $\sim 150 \mu\text{g}$. Calibration masses at this level are challenging to use. Their small size makes them delicate objects, difficult to manipulate, and as such, subject to damage from handling. Their force levels are comparable to forces from laboratory air currents, so calibrations need to be performed inside a draft shield and with many repetitions to reduce statistical uncertainty. This tedious process may be simplified, and its uncertainty significantly reduced from a manual method through the robotic automation described here.

3. CALIBRATION SCHEME

Commercial balances generally come with a calibration certification; however, factory calibrations are typically performed at mass values on the order of a gram (i.e., 5 orders of magnitude larger than the typical range of radiation pressure forces). For this reason, calibration with lower forces/masses is required due to potential instrument nonlinearity. To support current radiation pressure applications, our calibration procedure uses seven mass values from 163 μg to 48 mg corresponding to laser powers from 339 W to 100 kW at a 45° angle of incidence. As commercial force balances typically allow for measurement of much larger masses, they are well suited for laser powers in the hundreds of kilowatts regime, provided there are adequate mirror reflectivity and radiometer design. This illustrates one of the clear advantages of PMRs, as they are capable of a large dynamic range in power without the penalty of increased size and measurement support infrastructure.

PMR mass calibration artifacts are small sections of ultrafine wire. The wire thickness and length present a trade-off between mechanical robustness and suitability for robotic handling. Using aluminum and stainless-steel wire of diameter between 0.0635 and 0.508 mm, specialized mass artifacts have been designed. The artifacts are formed such that their mass is appropriate for the corresponding optical power level, and their shape

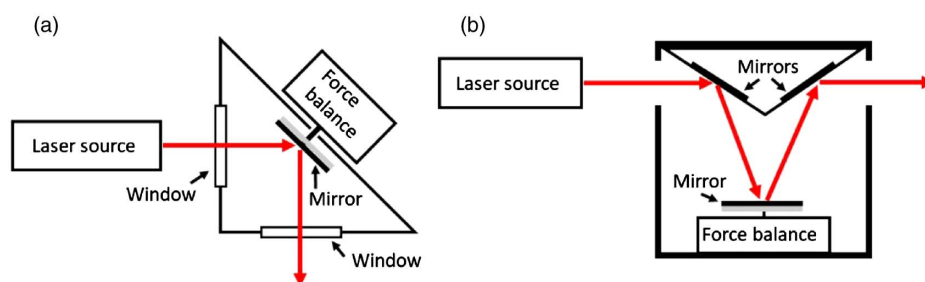


Fig. 1. Two different geometric configurations for measuring radiation pressure. In both cases the power in the laser beam is minimally perturbed for use after measuring the power in real time. (a) RPPM viewed from the top; (b) AFR viewed from the side.

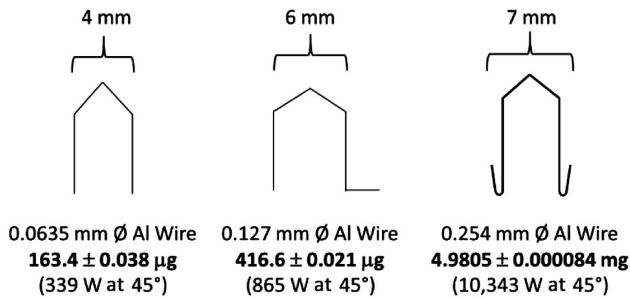


Fig. 2. Example of mass calibration artifacts. Calibration masses must be wide enough to be held when on the force sensor. The house-style shape allows for a low center of mass and easy placement on the calibrator robot arm. For each mass there are three parameters listed: the wire diameter used, the mass value, and the equivalent power level (a laser beam at this power level incident on a mirror at a 45° angle will produce a force that corresponds to the weight of the specified mass.)

facilitates mass placement automation. It is essential that the center of mass for each of the mass artifacts is sufficiently low for stability during robotic travel and placement. Mass artifacts with values as low as 0.05 mg have been produced commercially. It has been shown that these weights are stable over many years of use. Ultimately, mass design is limited by material selection and mass size [11]. Figure 2 illustrates a few of the masses currently used for calibration.

Masses are fabricated in-house and calibrated internally by the National Institute of Standards and Technology (NIST) Electrostatic Force Balance [12]. Masses are transported on the wire hook of a robotic arm and placed on a narrow two-pronged fork holder sitting on the force sensing balance pan [Fig. 3(a)]. As illustrated in Fig. 3(b), the width of each mass artifact must be large enough to span the custom “fork” on the mass holder that is placed on the force sensing pan. The holder is designed to minimize the weight on the force sensor while maintaining a robustness to prevent deformation upon continual mass loading. For current applications, a 0.2 mm thick copper sheet has been cut and folded to support the masses. Figure 3(a) also illustrates the mass hanging from the placement arm directly above the mass holder, and Fig. 3(c) roughly details the robotic delivery system that consists of multiple vertical translation elements for automated placement.

The robot is designed with a primary focus on consistent mass placement on the holder to reduce corner loading errors and balance hysteresis effects. Simple linear vertical travel is used for low cost, alignment, and ease of implementation in the control software. Although it has been shown that the interaction between the mass holders on the balance and the robot can lead to an additional bias force, measurements have shown that the bias force is small enough that the potential measurement bias is negligible at the combined expanded uncertainty of the comparable laser power measurement (i.e., 1.6%) [13]. However, for completeness, a two-axis pattern of travel was also tested to identify any unexpected static or magnetic effects from performing the tare weighing with the test mass suspended only a few millimeters above the force sensor. We found bias forces were present yet negligible, and thus simplified the repetitive process to merely vertical travel. The robot consists of a motorized linear actuator for mass placement, as well as a coarse manual linear travel adjustment along the same axis. The coarse travel is essential for alignment of the arm with the holder and accommodation of different force balance geometries. The actuator allows for up to 50 mm of travel, which is sufficient for mass placement. The coarse travel allows for 250 mm of travel, which accommodates a wide variety of commercial force balances, including the ones used in PMRs.

An enclosure is another essential component of the robotic calibrator setup. This minimizes external environmental effects on the system and limits contamination of the mass artifacts. Provided temperature stability is $23 \pm 3^\circ\text{C}$, thermal control is not required inside of this enclosure. Some form of closable port is necessary to allow access to place the mass artifact without risking loss or contamination.

4. RESULTS

Shifting from manual mass calibration processes to an automated method has allowed for more precise calibration. This is in part due to an increased number of measurements allowed by unattended operation and reduced measurement time (from typically 210 s per measurement when calibrating manually to 100 s per measurement when calibrating robotically). A significant advantage of the robotic operation is the ability to place and remove the mass without perturbing the force balance. In contrast, manual operation is likely to bump the mass holder during

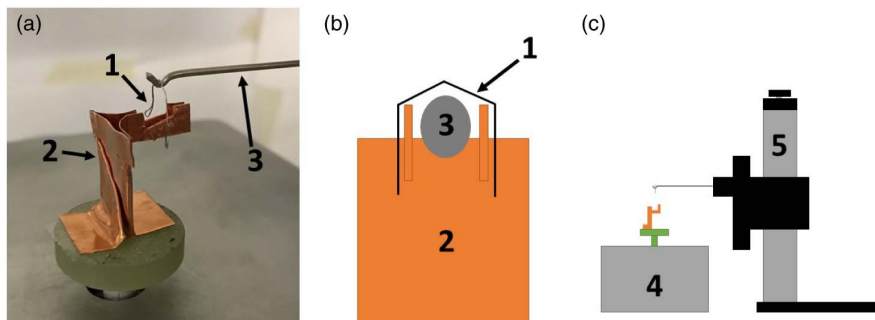


Fig. 3. Main components of the robotic mass placement system. (a) Closeup of operation with (1) mass artifact, (2) copper mass holder, and (3) robotic placement arm; (b) schematic view of dimensional relationship between elements: (1) mass artifact should be wide enough to straddle the acceptance arms of the (2) mass holder, which are in turn wider than the (3) robotic placement arm. (c) Relationship of the (4) force balance to the (5) robotic delivery stage.

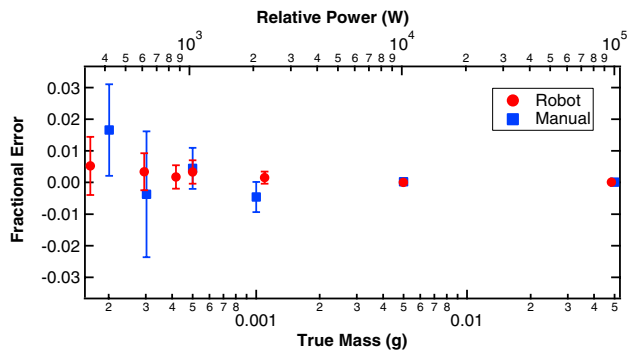


Fig. 4. Fractional error [Eq. (2)] as a function of true artifact mass for an RPPM force sensor, where squares represent a manual calibration (10 measurements per point) and circles represent a robotic calibration (35 measurements per point). For reference, the top axis indicates the laser power applied at normal incidence to a perfect reflector that would yield the same force as that produced by the mass value. Error bars represent 2 times the standard deviation of the mean (coverage factor, $k = 2$).

placement or removal, increasing the required settling time. This random perturbation also complicates automated analysis of the force sensor results. Once settling times for such perturbations are removed through data analysis, we measure roughly comparable standard deviations for manual and robotic operation. Faster measurements with the robotic approach, however, allow more data and a reduction in the statistical uncertainty on the measured mean mass. Figure 4 shows a direct comparison between two mass calibration routines, one performed by hand and the other with the robotic system. The data are plotted (Fig. 4) in terms of fractional error, which is denoted as

$$E_f = \frac{m_{\text{measured}} - m_{\text{true}}}{m_{\text{true}}}, \quad (2)$$

where m_{true} indicates the true mass obtained by the internal NIST Electrostatic Force Balance, and m_{measured} is the mean value obtained from the analytical balance. The error bars show statistical uncertainty only. This is dominated by the uncertainty in m_{measured} , calculated using the standard deviation of the mean of the m_{measured} values, with an expansion factor, $k = 2$ [14]. Figure 4 illustrates an offset introduced during manual calibration of the smallest masses. It can be seen that the fractional measurement uncertainty increases as the artifact mass is reduced. This is caused by environmental vibrational noise and electrical and mechanical limitations of the force balance, which are typically independent of measured mass, causing a reduced signal-to-noise ratio for smaller mass values. This is accounted for in the overall PMR device uncertainty. Testing with the robotic setup yielded smaller fractional error and measurement uncertainty. Notably, this balance appears linear within 1% across 3 orders of magnitude, which is not necessarily guaranteed for such instrumentation.

For comparison, Fig. 5 shows robotic calibration results for a different balance. The increased precision of the robotic calibration allows us to demonstrate measurement errors outside of the statistical uncertainty, permitting us to correct for it. The fractional error data are fit with a third-order polynomial. The fit coefficients generated are then input into the custom

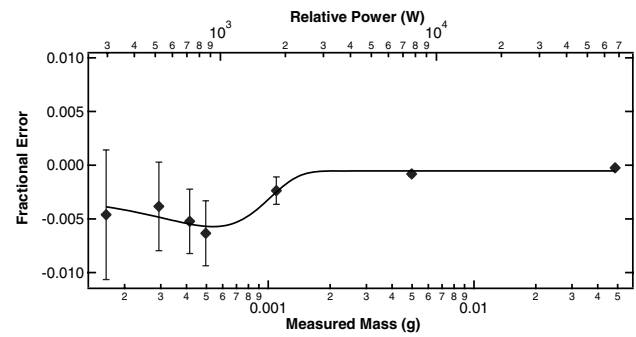


Fig. 5. Data from an AFR force sensor, representing fractional error as a function of measured mass by the balance. The top axis again provides reference for a laser power on a perfect reflector at normal incidence that would yield the same force as that produced by the mass value. The calculated curve fit used to correct the balance readout is shown as well. Error bars represent 2 times the standard deviation of the mean (coverage factor, $k = 2$).

software routine that automatically interpolates and corrects the balance readout in real time in accordance with the robotic calibration results. The data for the balance in Fig. 5 also illustrate an improvement in fractional error for a robotic calibration procedure. The same measurement done without automation had a statistical uncertainty larger than the fractional error (preventing software correction of the balance reading).

Automation generates several improvements to the calibration procedure. One benefit is increased stability in the calibration environment. Previously, the user had to locate, grasp, and place each artifact on the force sensor for each measurement. Effects such as air currents and variations in humidity and temperature due to manual handling degrade balance performance, particularly in the case of operator error (bumping the pan, for example) during placement or removal of the mass artifact. The robotic method allows for the process to be completely isolated in an enclosure during the measurement, which greatly reduces environmental disturbances to the balance operation. Another improvement with automation is the reduced user contact with the mass artifacts. Given that the artifacts are constructed from very thin wire, handling results in bending and potential damage to the masses. With the current robotic calibration system, the mass only needs to be placed on the arm at the start of the calibration run and removed at the end. This reduces wear and tear on the mass and reduces the amount of time the operator spends on the calibration. Analysis of the data has also been simplified due to reduced user interaction, with the balance allowing for less user interaction in analysis as well.

5. CONCLUSIONS

Radiation pressure as a means for high-power laser power measurement allows traceability to the fundamental constants through the meter, kilogram, and second. Multiple device geometries and force sensors for PMR devices can be accurately calibrated using traceable mass artifacts. Robotic calibration techniques have been implemented for these measurements and yield multiple benefits. The uncertainty of the procedure is sufficiently low that a correction calibration curve may be assigned

to a commercially available analytical balance for the application of photon momentum. Increased sample sizes produce smaller statistical uncertainty, and isolated calibration conditions allow for minimal external disturbances. Automation of mass handling also prevents mass contamination or damage and reduces the time burden on the operator. Decrease in statistical uncertainty from the robotic calibration also allows for us to quantify variations in the measured fractional error previously within the measurement uncertainty, thereby improving the accuracy of the PMR.

Funding. Naval Surface Warfare Center.

Disclosures. The authors declare no conflicts of interest.

Supplementary Material

See [Supplement 1](#) for supporting content.

REFERENCES

1. P. Williams, J. Hadler, F. Maring, R. Lee, K. Rogers, B. Simonds, M. Spidell, M. Stephens, A. Feldman, and J. Lehman, "Portable, high-accuracy, non-absorbing laser power measurement at kilowatt levels by means of radiation pressure," *Opt. Express* **25**, 4382–4392 (2017).
2. P. A. Williams, M. T. Spidell, J. A. Hadler, T. Gerrits, A. Koepke, D. Livigni, M. S. Stephens, N. A. Tomlin, G. A. Shaw, J. D. Splett, I. Vayshenker, M. G. White, C. S. Yung, and J. H. Lehman, "Meta-study of laser power calibrations ranging 20 orders of magnitude with traceability to the kilogram," *Metrologia* **57**, 015001 (2019).
3. I. A. Robinson and S. Schlamminger, "The watt or Kibble balance: a technique for implementing the new SI definition of the unit of mass," *Metrologia* **53**, A46–A74 (2016).
4. G. A. Shaw and J. Stirling, "Measurement of submilligram masses using electrostatic force," *IEEE Trans. Instrum. Meas.* **68**, 2015–2020 (2019).
5. X. Li, J. A. Hadler, C. L. Cromer, J. H. Lehman, and M. L. Dowell, *NIST Measurement Services: High Power Laser Calibrations at NIST*. Vol. 250-77 of NIST Special Publication (National Institute of Standards and Technology, 2008), pp. 250–277.
6. P. Williams, A. Artusio-Glimpse, J. Hadler, D. King, T. Vo, K. Rogers, I. Ryger, and J. Lehman, "Radiation-pressure enabled traceable laser sources at CW powers up to 50 kW," *IEEE Trans. Instrum. Meas.* **68**, 1833–1839 (2019).
7. P. A. Williams, J. A. Hadler, B. J. Simonds, and J. H. Lehman, "Onsite multikilowatt laser power meter calibration using radiation pressure," *Appl. Opt.* **56**, 9596–9600 (2017).
8. J. Lehman, K. Rogers, D. Rahn, and P. Williams, "Inline laser power measurement by photon momentum," *Appl. Opt.* **58**, 1239–1241 (2019).
9. P. A. Williams, K. A. Rogers, J. A. Hadler, A. B. Artusio-Glimpse, and J. L. Lehman, "Axial force radiometer for primary standard laser power measurements using photon momentum," *Metrologia* (to be published).
10. D. R. Tate, *Acceleration Due to Gravity at the National Bureau of Standards* Vol. 107 of National Bureau of Standards Monograph (National Bureau of Standards, 1967), pp. 1–20.
11. "Test Weights and Calibration Weights," 2020, https://www.mt.com/us/en/home/library/white-papers/laboratory-weighing/08_Weights/WP_Weights_Traceability_Microgram_Request.html.
12. G. A. Shaw, J. Stirling, J. A. Kramar, A. Moses, P. Abbott, R. Steiner, A. Koffman, J. R. Pratt, and Z. J. Kubarych, "Milligram mass metrology using an electrostatic force balance," *Metrologia* **53**, A86–A94 (2016).
13. J. R. Pratt and J. A. Kramar, "SI realization of small forces using an electrostatic force balance," *Proc. XVIII IMEKO World Congress on Metrology for a Sustainable Development*, Rio de Janeiro, Brazil, 17–22 September (2006), p. 109.
14. "Evaluation of measurement data—guide to the expression of uncertainty in measurement (GUM 1995 with minor corrections," JCGM 100:2008 (Joint Committee for Guides in Metrology, 2008).